Published in final edited form as:
J Neurooncol. 2015 January ; 121(1): 109–118. doi:10.1007/s11060-014-1618-8.

EphrinB1 expression is dysregulated and promotes oncogenic signaling in medulloblastoma

Nicole McKinney[1], **Liangping Yuan**[1], **Hongying Zhang**[1], **Jingbo Liu**[1], **Yoon-Jae Cho**[2], **Elisabeth Rushing**[3], **Matthew Schniederjan**[4], and **Tobey J. MacDonald**[1]

[1]Department of Pediatrics, Aflac Cancer and Blood Disorders Center, Emory University School of Medicine, Atlanta, GA 30322, USA [2]Departments of Neurology and Neurological Sciences, Stanford University School of Medicine, Stanford, CA 94305, USA [3]Institute of Neuropathology, University Hospital of Zurich, Schmelzbergstr, 12, CH-8091 Zurich, Switzerland [4]Department of Pathology, Emory University School of Medicine, Atlanta, GA 30322, USA

Abstract

Eph receptors and ephrin ligands are master regulators of oncogenic signaling required for proliferation, migration, and metastasis. Yet, Eph/ephrin expression and activity in medulloblastoma (MB), the most common malignant brain tumor of childhood, remains poorly defined. We hypothesized that Eph/ephrins are differentially expressed by sonic hedgehog (SHH) and non-SHH MB and that specific members contribute to the aggressive phenotype. Affymetrix gene expression profiling of 29 childhood MB, separated into SHH (N=11) and non-SHH (N=18), was performed followed by protein validation of selected Eph/ephrins in another 60 MB and two MB cell lines (DAOY, D556). Functional assays were performed using MB cells overexpressing or deleted for selected ephrins. We found *EPHB4* and *EFNA4* almost exclusively expressed by SHH MB, whereas *EPHA2, EPHA8, EFNA1* and *EFNA3* are predominantly expressed by non-SHH MB. The remaining family members, except *EFNB1*, are ubiquitously expressed by over 70–90% MB, irrespective of subgroup. *EFNB1* is the only member differentially expressed by 28% of SHH and non-SHH MB. Corresponding protein expression for EphB/ephrinB1 and B2 was validated in MB. Only ephrinB2 was also detected in fetal cerebellum, indicating that EphB/ephrinB1 expression is MB-specific. EphrinB1 immunopositivity localizes to tumor cells within MB with the highest proliferative index. EphrinB1 overexpression promotes EphB activation, alters F-actin distribution and morphology, decreases adhesion, and significantly promotes proliferation. Either silencing or overexpression of ephrinB1 impairs migration. These results indicate that EphrinB1 is uniquely dysregulated in MB and promotes oncogenic responses in MB cells, implicating ephrinB1 as a potential target.

Address correspondence to: Tobey J. MacDonald, Emory Children's Center, Aflac Cancer and Blood Disorders Center, 2015 Uppergate Drive NE, 4th Floor, Atlanta, GA 30322. Telephone: 404-727-1447, Fax: 404-727-4455, tobey.macdonald@emory.edu.

Ethical standards

The experiments comply with the current laws of the country in which they were performed.

Conflict of interest

The authors declare that they have no conflict of interest.

Keywords

EphrinB1; dysregulation; medulloblastoma; oncogenic signaling

Introduction

Medulloblastoma (MB), an invasive embryonal tumor of the cerebellum, is the most common malignant brain tumor in children [1]. Standard treatment includes whole brain irradiation for the prevention of metastasis; however, this carries a high risk of neurocognitive morbidity and is suboptimal treatment for pre-existing metastases [1]. Identifying the key molecular contributors to MB aggressiveness should yield more effective and less toxic tumor-targeted therapy.

Potential candidates for promoting MB metastasis include the Eph receptor protein tyrosine kinases and their ephrin ligands. Eph-ephrin complexes emanate bidirectional signals via cell-cell contacts: forward signals depend on Eph kinase activity in the Eph-expressing cell and reverse signal propagation depends on Src kinases in the ephrin-expressing cell [2]. Signaling can also be mediated by ephrins independent of Eph kinase activity [3, 4]. Eph signaling regulates migration and invasion through re-organization of the actin cytoskeleton and by impacting the activities of intercellular adhesion molecules [5, 6]. In humans, there are 9 EphA receptors, which promiscuously bind 5 GPI-linked ephrinA ligands, and 5 EphB receptors, which promiscuously bind 3 transmembrane ephrinB ligands [6]. Exceptions are the EphA4 and EphB2 receptors, which can bind ephrinBs and ephrinA5, respectively, and EphB4, which preferentially binds ephrinB2.

Eph-ephrin complexes promote adhesiveness, while the removal of these complexes from cell contact sites produces repulsive responses. Eph-dependent repulsive and adhesive forces can drive the segregation of cell populations expressing different repertoires of Eph receptors and ephrins [7–8]. For example, ephrinB loss results in the inability of the Reelin pathway to regulate neuronal cell migration in the developing cerebellum [9]. Animal models lacking Eph receptor expression also show impairment of normal cerebellar development [10–13].

Essentially all cancer cells express Eph receptors and/or ephrins and the expression levels correlate with metastasis and patient survival [14, 15]. Eph receptors and ephrins have been shown to affect tumor growth, invasiveness, angiogenesis, and metastasis *in vivo* [16, 17]; however, the expression and function of Eph/ephrins in MB remains ill-defined. Several published datasets provide evidence for expression of *Eph/ephrins* associated with the four MB subgroups: WNT, Sonic hedgehog (SHH), Group 3 and Group 4 [18–21]. However, deciphering the functional role of Eph/ephrins is difficult given that increased and decreased expression has been linked to cancer progression, and that Eph/ephrins can both promote and inhibit tumorigenicity [6, 10, 16]. The aim of this study was to better define the expression of Eph/ephrins in MB and to identify the leading candidates for promoting the aggressive phenotype typically observed in non-WNT MB.

Materials and Methods

Cells and reagents

DAOY and D556, two validated human medulloblastoma cells, were used for investigation [20].

Patient tissue specimens

Twenty-nine fresh-frozen medulloblastoma (MB) specimens were acquired from the Children's Healthcare of Atlanta (CHOA) tumor tissue repository. Normal fetal cerebellar tissue was obtained from Emory University Hospital Department of Pathology. Tissue microarrays were constructed from 60 parrafin-embedded MB obtained from AFIP Pathology and reviewed by two board-certified neuropathologists (MS, ER). The research protocols were approved by the institutional review boards of CHOA, Emory University, and AFIP. All tissue specimens were consented for and de-identified.

Microarray gene expression profiling

RNA was extracted from 29 frozen MB using Trizol (Invitrogen, Carlsbad, CA) and profiled by AROS Biosciences on the Affymetrix human genome U133 Plus 2.0 array with the 3′ IVT Express Labeling Kit (Affymetrix, Santa Clara, CA). Relative mean expression levels for each gene were calculated by the Affymetric microarray software. CEL files were preprocessed using RMA and probeset collapsed to genes using the Genepattern software suite (www.broadinstitute.org/cancer/software/genepattern/) [22]. Samples were then assigned to molecular subgroups as previously described, using a classifier based on support-vector machines [23].

Western blot

Western blot of whole cell lysates was performed using the primary antibodies, EphB1, EphB2, ephrinB1, ephrinB2, phospho-EphB1/B2 (Abcam, Cambridge MA), phospho-Src and GADPH (Cell Signaling Technology, Danvers, MA) and goat or rabbit anti-mouse horseradish peroxidase secondary antibodies (Santa Cruz, CA). Each blot is representative of at least three separate experiments.

Immunohistochemistry

Immunohistochemistry (IHC) was performed using the primary antibodies, EphB1, EphB2 (Abcam, Cambridge MA), ephrinB1, ephrinB2 (R&D Systems, Minneapolis MN), and ephrinA3 (Antibodies Onlines, Atlanta GA) and tissue microarrays (TMA) comprised of 60 MB. Negative and positive controls were normal fetal cerebellum and tumor tissues expressing the corresponding Eph/ephrins, including breast carcinoma (Abcam, Cambridge MA), respectively. Incubation with anti-Eph or -ephrin (1:150 dilution) was performed overnight at 4°C and immunodetection was performed using the Elite Vectastain ABC system (Vector Laboratories, Burlingame, CA). Color visualization was performed using 3, 3′-diaminobenzide as the chromagen substrate (Innovex Biosciences, Pinole, CA). Haematoxylin was used as the counterstain. Each tissue sample was independently scored for positivity by two neuropathologists (ER or MS). Scoring was performed blinded and the

immunostaining results were graded as either negative or positive. The grading definitions used were established by the neurophathologists based on the relative diffuse cellular homogeneity observed for the specific target staining tested.

EphrinB siRNA transfection

EphrinB1 and ephrinB2 siRNA (166144F04 and163363D02) and negative control non-targeting siRNA (12935-200) were purchased from Invitrogen (Grand Island, NY). For transfections, 1.2×10^5 cells were seeded in each well of a six-well plate and grown to 50–60% confluency prior to transfection. Cells were transfected with siRNA using Lipofectamine 2000 (Invitrogen, Carisbad, CA) for 48 h according to the manufacturer's instruction. The final concentration of siRNA was 100 nmol/l. Western blots were used to verify ephrinB1 expression.

EphrinB1 stable transfection

1.5×10^5 cells were seeded in 6-well plates and 5 ug of plasmid containing ephrinB1(Origene Technologies, Rockville MD) was mixed with varying amounts (7.5–20 uL) of turbofectamine transfection reagent (Origine Technologies, Rockville MD) in 200 µl OPTI-MEM solution. 48h later, cells were split into a 75 cm^2 flask and treated with G418 and then passaged several times under selective G418. Western blots were used to verify stable ephrinB1 overexpression.

F-actin immunofluorescence

Cells grown on glass coverslips (Fisher) coated with 5 $\mu g/cm^2$ fibronectin (Chemicon International) in a 24-well plate were fixed with PHEMO buffer (68 mM PIPES, 25 mM HEPES, 15 mM $EGTANa_2$, 3 mM $MgCl_26H_2O$, 10% DMSO, pH 6.8) supplemented with 3.7% formaldehyde (Fisher), 0.05% glutaraldehyde (Fisher) and 0.5% Triton X-100 (Fisher) and washed with PBS and blocked for 10–15 min in 10% goat serum (Cellgro). Actin was labeled by staining with Alexa Fluor 555 phalloidin (Invitrogen) at 1:40 in PBS and DNA was stained with 300 nM 4′-6-diamidino-2-phenylinodle, dilactate (DAPI, Invitrogen) for 5–10 min in dH_2O. Coverslips were mounted on microslides (Fisher) using 20–30 µl polyvinyl alcohol mounting media with DABCO anti-fade (Fluka) and allowed to dry overnight at room temperature. Morphology was determined by visualizing cells using a point scanning laser confocal microscope (LSM 510 META) and analyzing cell length and cell footprint area using Zeiss Image Browser's region of interest tool (ROI).

Cell adhesion assay

Harvested cells were resuspended in 10% FBS containing EMEM (2.5 × 10e5 cells/ml) and 2ml of suspension was added to each well of a 6-well plate coated with either fibronectin or collagen, and incubated for 30 min at 37°C. The assay was stopped by rinsing cells with PBS x 3. Cells were fixed and stained with 700 ml of staining solution (Chemicon International, Temecula, CA) and washed. Cells were eluted with extraction solution and 100 uL transferred to a 96-well microtiter plate for absorbance reading at 570 nm. Each experiment was performed at least three separate times.

Cell viability and proliferation assays

Cell viability and proliferation was measured by cell counting using trypan blue exclusion and MTT assay, respectively. For the MTT assays, cells (1500 cells/well) were seeded into 96-well microplates. After 24h incubation, 10 uL of MTT reagent (consisting of 5mg Thiazolyl Blue Tetrazolium Bromide per 10 ml PBS) was added to each well, and incubated for 4h at 37°C. 100 uL of 0.04% HCl in isopropanaolol was added to each well and the spectrophotometric absorbance was measured at 570 nm using a Synergy Mx microplate reader. Each experiment was performed at least three separate times.

Cell migration and motility assays

Cell migration and motility was measured by scratch assay and real-time video microscopy, respectively. For scratch assays, cells (2.5×10^5/well) were seeded in 6-well plates, with or without fibronectin or collagen, and incubated overnight at 37°C. A p1000 pipet tip was used to scrape the cell monolayer to create a “scratch” and growth medium replenished. Corresponding scratches were photographed under light microscopy at time 0, 24, and 48h. Scratch widths at each time point were measured manually with changes in widths calculated over the first 24 hour period to avoid the impact of proliferation between 24–48 hours. Each experiment was performed at least three separate times.

To capture images of single cell motility, a Perkin Elmer Ultraview ERS spinning disc confocal microscope was used. The confocal scanner is mounted onto a Zeiss Axiovert II microscope encased at 37°C with CO_2 perfusion. Cells were plated on fibronectin-coated live cell imaging plates (Lab-Tek) and images were captured using a Zeiss 10x Plan-Neofluar objective (NA = 0.3). Images were acquired using a Hamamatsu ORCA ER CCD camera every 10 min for 24 h at multiple z-planes. A motorized ASI stage was used to acquire images at multiple x and y coordinates throughout the sample. Image analysis was performed by manually tracking cells using Volocity software (Perkin Elmer).

Statistical analysis

For all pair-wise comparisons, results are analyzed using a 2-tailed Student’s t test. Values of $P < .05$ are considered to be statistically significant.

Results

Eph receptors and ephrin ligands are differentially expressed by MB

The mRNA expression data for *EPHs* and *EFNs*, and the accompanying histopathologic and clinical data, are provided in Online Resource 1. Profiles were compared with respect to sonic hedgehog (SHH) vs. non-SHH (Group 3 and 4). SHH tumors were further subdivided between desmoplastic histology, typically seen in infants and associated with good prognosis, and non-desmoplastic histology, which is seen more commonly in older children and is associated with an intermediate prognosis [24]. Expression of *EPHA1, EPHA6* and *EPHB3* was not detected. *EFNA4* and *EPHB4* are almost exclusively expressed by SHH MB, whereas *EFNA1, EFNA3, EPHA2, EPHA8* are predominantly expressed in non-SHH MB. In contrast, the percentage of tumors with detectable expression, and the relative mean expression level, for SHH and non-SHH tumors is nearly identical for *EFNB1, EFNB2,*

EFNB3, *EPHB1*, *EPHB2*, and *EPHB6*. There was no detectable difference in the expression of any member between Group 3 and 4 tumors of the non-SHH MB sub-group.

Because of the relatively uniform expression in SHH and non-SHH MB for the functionally-interacting pairs, *EPHB1* and *EPHB2* with *EFNB2* and *EFNB1*, we focused on these specific family members for further characterization by protein expression in 60 additional MB and in two human MB cell lines, as shown in Online Resource 2. D556 cells are positive for EphB1/B2 and ephrinB1/B2 protein, while Daoy cells are also positive for each member, but equivocal for EphB1. As expected from the mRNA data, we detected positive protein expression for EphB1, EphB2 and ephrinB2 in over 95% MB, while ephrinB1 was detected in 15% MB. EphB1, EphB2 and ephrinB2 stained diffusely and densely positive in nearly every tumor analyzed, as did ephrinA3, a minor ligand for EphB1, while ephrinB1 strikingly showed positive staining that was primarily localized to the regions within the tumors containing more densely populated neoplastic cells displaying a higher MIB proliferative index associated with aggressive phenotypes (Fig. 1). Of these targets, only ephrinB2 was also detected in the developing fetal cerebellum, with positive expression restricted to the purkinje cells (data not shown), indicating that EphB1/B2 and ephrinB1 expression is tumor-specific (Fig. 1). Although ubiquitously expressed in MB, ephrinB2 does not appear to be overexpressed, and thus because of its positive staining in normal cerebellum, we believe ephrinB2 to be more indicative of normal rather than oncogenic Eph/ephrin signaling.

EphrinB1 and ephrinB2 differentially regulate EphB1/B2 and Src activation in MB cells

It has been demonstrated that Eph-ephrin signal transduction can occur through recruitment and activation of Src [25, 26]. Therefore, we were interested in determining whether EphB receptor forward signaling activation in MB cells is dependent on specific ephrinB ligand interaction and whether specific ephrinBs can induce Src activation that is typically required for mediating reverse signaling. To address these questions, we knockdown ephrinB1 and ephrinB2 and then examined the phosphorylation of EphB1/B2 and Src compared to control transfected cells. With silencing of ephrinB1, we observed a modest decrease in the level of phosphorylated (p)-EphB1/B2, but no change in the level of p-Src (Fig. 2a). In contrast, ephrinB2 silencing resulted in a marked decrease in the level of p-EphB1/B2 and a concomitant reduction in the level of p-Src (Fig. 2b), as would be expected in normal ephrin-mediated reverse signaling.

To confirm that ephrinB1 directly modulates EphB1/B2 phosphorylation, we overexpressed ephrinB1. In comparison to control cells, ephrinB1 overexpression increased EphB1/B2 phosphorylation, but did not change Src phosphorylation or the total level of the EphB1 receptor (Fig. 2b). For all signaling studies, similar results were obtained in both D556 (shown) and Daoy (Online Resource 5) cell types.

EphrinB1-mediated activation of EphB signaling regulates cell morphology, F-actin distribution, adhesion, proliferation, migration and motility of MB cells

EphB-mediated signaling can result in either tumor promoting or tumor inhibitory cellular responses. Thus, to identify the functional role of ephrinB1-mediated activation of EphB

signaling activity in MB cells, we investigated the effect of altered ephrinB1 expression on MB cell morphology, F-actin distribution, adhesion, proliferation, migration and motility.

In contrast to MB cells plated on fibronectin, which display a morphology characterized by cell spreading in monolayers to form cell-cell contacts, ephrinB1 overexpressing MB cells grown on fibronectin display strikingly contracted cells growing in segregated colonies (Fig. 3a). Cells with ephrinB1 overexpression showed a clear change in the cellular distribution of F-actin, predominantly exhibiting a ring-enhancing pattern that was consolidated at the periphery of the cell membrane, suggesting a rearrangement in focal adhesion sites, while control cells demonstrated diffusely aligned F-actin distribution (Fig. 3b).

The morphologic and F-actin distribution changes in ephrinB1 overexpressing cells were associated with a concomitant decrease in cell adhesion to fibronectin ($p<0.001$) and collagen ($p<0.001$)) (Fig. 4). EphrinB1 overexpression also resulted in a significant increase in cell viability and proliferation as measured by cell counting and MTT assay ($p=0.006$, Online Resource 3). We were unable to propagate stable ephrinB1 knockdown cells for analysis by MTT assay, suggesting that ephrinB1 is critical for cell replication in culture. EphrinB2 knockdown cells appeared to show a trend towards inhibition of proliferation compared to control cells, but this did not quite reach significance ($p=0.08$, data not shown), in keeping with the concept that ephrinB2 acts more as a regulator of normal, rather than oncogenic, Eph/ephrin signaling. Because of this result, coupled to its positive staining in normal cerebellum, we elected not to further test the impact of ephrinB2 knock-down on other MB cell responses.

Finally, ephrinB1 knock-down resulted in a significant decrease in cell migration and motility ($p=0.01$) compared to control transfected cells, as measured by scratch assay (Fig. 5a) and real-time video microscopy (Fig. 5b). Interestingly, ephrinB1 overexpression also significantly impaired cell motility on fibronectin, with cells showing a decrease in cell velocity ($p=0.01$, Online Resource 4) and an increase in non-directed cell meandering ($p=0.05$) compared to control cells, suggesting that a critical balance in ephrinB1 expression and activity is necessary to maintain optimal migration capacity. For all cellular response studies, similar results were obtained in both D556 (shown) and Daoy (Online Resource 5) cell types.

Discussion

Evidence implicates Eph receptors as master regulators in cancer cells; capable of potentiating or suppressing oncogenic signaling depending on the specific ephrin ligand interaction and the resultant bidirectional signaling [5, 6, 10, 16]. In a number of malignancies, including adult brain tumors, Eph and ephrin expression is dysregulated and correlates with cancer progression, metastatic spread and patient survival [27, 28]. However, only limited information exists for Eph-ephrins in medulloblastoma (MB). Herein, we present the most complete characterization of Eph/ephrins expression in MB, and in doing so, identify a unique tumor-specific pattern of expression for ephrinB1. First, analysis of two independent tumor cohorts revealed that ephrinB1 overexpression is observed in a subset of MB (~30% by mRNA and ~15% by protein, respectively), whereas the positive mRNA and

protein expression detected for all the other Eph family members investigated is ubiquitous (>90% of all MB), or primarily associated with either SHH or non-SHH type MB. Because of this unique expression pattern, we postulated that ephrinB1 could be a clinically targetable biomarker for the ~15–30% of highly aggressive MB that are refractory to standard treatment. Although our tumor cohorts are too small to confirm clinical associations, we noted in large public datasets of MB gene expression that ephrinB1 overexpression is associated with Group 3 MB [18, 19], which typically has the highest rates of metastasis and comprises a large percentage of refractory MB. Furthermore, we found the combined positive protein expression of EphB1, EphB2, and ephrinB1 only in MB, and not in normal fetal cerebellum, confirming expression is tumor-specific. However, whereas EphB1 and EphB2 are diffusely expressed in MB, ephrinB1 is primarily restricted to the highly proliferative and dense cellular areas within the tumor associated with the most aggressive phenotypes, suggesting that ephrinB1 may have a separate and specific oncogenic role.

Indeed, we provide compelling evidence in support of a primary oncogenic role for ephrinB1-mediated signaling in MB cells (D556 and Daoy), by showing that ephrinB1 overexpression significantly enhances cell viability and proliferation while promoting cell adhesion, motility, migration, as well as the morphology and F-actin distribution pattern that is characteristic of the aggressive cancer phenotype. However, the cellular responses were not associated with a concomitant change in EphB kinase activity, indicating that ephrinB1-mediated reverse signaling, independent of EphB kinase-mediated forward signaling, is responsible for the changes we observed in these MB cells, as has been described in other cell types [3, 4]. Furthermore, and in contrast to ephrinB2, alterations in ephrinB1 expression did not impact downstream Src activity, as is commonly seen in normal ephrin-mediated reverse signaling. Together, these results indicate that ephrinB1 mediates a unique signaling pathway in MB cells that is clearly outside of the traditional EphB/ephrinB signaling axis. By comparison, ephrinB2, which is expressed by normal cerebellum and does not significantly impact MB cell proliferation, demonstrated a more normal cell signaling pattern through the Eph/ephrin axis. Yet, we also show that optimal activation of EphB1/B2 forward signaling is dependent on concomitant interaction with ephrinB1 and/or B2, and thus ephrinB1 and ephrinB2 also function to promote signaling within the classic EphB1/B2 pathway. These results have important clinical implications, as it suggests that dual targeting of Eph and ephrin within the complex may be necessary to fully impact oncogenic signaling.

EphrinB1 signaling induces invasion of glioma, pancreatic, gastric and leukemic cancer cells *in vitro* and in mouse tumor models [29–31]. And expression of *EphB2* and *ephrinB1* was shown to be significantly increased in MB [21]. However, in contrast to our study, ephrinB1-induced migration and invasion was ablated by knocking-down EphB2 [21]. In our study, ephrinB1 signaling promotes oncogenic responses that are seemingly independent of either EphB or Src activation, yet the mechanism remains to be elucidated. In glioma cells, Src-mediated ephrinB1 phosphorylation promotes RAC1-dependent invasion [32, 33], while suppression of ephrinB1 signaling in malignant T lymphocytes inhibits invasiveness [29]. Stimulation of EphB2 signaling with ephrinB1-Fc in colon carcinoma cells increased intercellular adhesion by promoting membrane localization of E-cadherin [34], but in

colorectal cells lacking E-cadherin, a pro-repulsive response was observed [35]. In epithelial cells, ephrinB1 associates with the Par polarity complex protein Par-6, a scaffold protein required for establishing tight junctions, and can compete with the small GTPase Cdc42 for association with Par-6. This competition causes inactivation of the Par complex, resulting in the loss of tight junctions [36]. Interestingly, phosphorylated ephrinB1 can also bind and directly activate STAT3, a transcription factor involved in cancer progression [37], suggesting yet another possible mechanism by which ephrinB1 could promote oncogenic signaling in MB cells independent of EphB or Src. Because of our observed impact of ephrinB1 on MB cell propagation, further delineation of the possible association of ephrinB1 with the stem cell niche, as well as the signaling and functional roles of the EphB receptors and corresponding ephrinB ligands in preclinical investigation of MB *in vivo*, is warranted in order to validate these members as potential novel therapeutic targets in MB.

Supplementary Material

Refer to Web version on PubMed Central for supplementary material.

Acknowledgments

Video microscopy results were obtained using the Integrated Cellular Imaging (ICI) Core Facility, Emory University Winship Cancer Institute. Funding support provided in part by National Institute Health R01CA111835 (TJM), CURE Childhood Cancer (NM), and the Georgia Research Alliance (TJM).

References

1. Crawford JR, MacDonald TJ, Packer RJ. Medulloblastoma in childhood: new biological advances. Lancet Neurol. 2007; 6:1073–1085. [PubMed: 18031705]
2. Palmer A, Zimmer M, Erdmann KS, Eulenburg V, Porthin A, et al. EphrinB phosphorylation and reverse signaling: Regulation by Src kinases and PTP-BL phosphatase. Mol Cell. 2002; 9:725–737. [PubMed: 11983165]
3. Gu C, Park S. The EphA8 receptor regulates integrin activity through p110gamma phosphatidylinositol-3 kinase in a tyrosine kinase activity-independent manner. Mol Cell Biol. 2001; 21:4579–4597. [PubMed: 11416136]
4. Miao H, Strebhardt K, Pasquale EB, Shen TL, Guan JL. Inhibition of integrin-mediated cell adhesion but not directional cell migration requires catalytic activity of EphB3 receptor tyrosine kinase. Role of Rho family small GTPases. J Biol Chem. 2004; 280:923–932. [PubMed: 15536074]
5. Pasquale EB. Eph-ephrin bidirectional signaling in physiology and disease. Cell. 2008; 133:38–52. [PubMed: 18394988]
6. Paquale EB. Eph receptor signalling casts a wide net on cell behaviour. Nat Rev Mol Cell Biol. 2005; 6:462–475. [PubMed: 15928710]
7. Kemp HA, Cooke JE, Moens CB. EphA4 and EfnB2a maintain rhombomere coherence by independently regulating intercalation of progenitor cells in the zebrafish neural keel. Devel Biol. 2009; 327:313–326. [PubMed: 19135438]
8. Batlle E, Bacani J, Begthel H, Jonkheer S, Gregorieff A, et al. EphB receptor activity suppresses colorectal cancer progression. Nature. 2005; 435:1126–1130. [PubMed: 15973414]
9. Sentürk A, Pfennig S, Weiss A, Burk K, Acker-Palmer A. Ephrin Bs are essential components of the Reelin pathway to regulate neuronal migration. Nature. 2011; 472:356–360. [PubMed: 21460838]
10. Kullander K, Klein R. Mechanisms and functions of Eph and ephrin signalling. Nat Rev Mol Cell Biol. 2002; 3:475–486. [PubMed: 12094214]
11. Akay T, Acharya HJ, Fouad K, Pearson KG. Behavioral and electromyographic characterization of mice lacking Eph A4 receptors. J Neurophysiol. 2006; 96:642–651. [PubMed: 16641385]

12. Dottori M, Hartley L, Galea M, Paxinos G, Polizzotto M, et al. EphA4(Sek1) receptor tyrosine kinase is required for the development of the corticospinal tract. Proc Natl Acad Sci. 1998; 95:13248–13253. [PubMed: 9789074]
13. Miko I, Henkemeyer M, Cramer K. Auditory brainstem responses are impaired in EphA4 and ephrin-B2 deficient mice. Hear Res. 2008; 235:39–46. [PubMed: 17967521]
14. Dong Y, Wang J, Sheng Z, Li G, Ma H, et al. Downregulation of EphA1 in colorectal carcinomas correlates with invasion and metastasis. Mod Pathol. 2009; 22:151–160. [PubMed: 19011600]
15. Jubb AM, Zhong F, Bheddah S, Grabsch HI, Frantz GD, et al. EphB2 is a prognostic factor in colorectal cancer. Clin Cancer Res. 2005; 11:5181–5187. [PubMed: 16033834]
16. Campbell TN, Robbins SM. The Eph receptor/ephrin system: an emerging player in the invasion game. Curr Issues Mol Biol. 2008; 10:61–66. [PubMed: 18525107]
17. Petty A, Myshkin E, Qin H, Guo H, Miao H, et al. A small molecule agonist of EphA2 receptor tyrosine kinase inhibits tumor cell migration in vitro and prostate cancer metastasis in vivo. PLoS One. 2012; 7:e42120. [PubMed: 22916121]
18. Northcott PA, Korshunov A, Witt H, Hielscher T, Eberhart CG, et al. Medulloblastoma comprises four distinct molecular variants. J Clin Oncol. 2011; 29:1408–1414. [PubMed: 20823417]
19. Kool M, Koster J, Bunt J, Hasselt NE, Lakeman A, et al. Integrated genomics identifies five medulloblastoma subtypes with distinct genetic profiles, pathway signatures and clinicpathological features. PLoS One. 2008; 3:1–14.
20. MacDonald TJ, Brown K, LaFleur B, Peterson K, Lawlor C, et al. Expression profiling of medulloblastoma: PDGFRA and the RAS/MAPK pathway as therapeutic targets for metastatic disease. Nat Genet. 2001; 29:143–152. [PubMed: 11544480]
21. Sikkema AH, den Dunnen WF, Hulleman E, van Vuurden DG, Garcia-Manero G, et al. EphB2 activity plays a pivotal role in pediatric medulloblastoma cell adhesion and invasion. Neuro Oncol. 2012; 14:1125–35. [PubMed: 22723427]
22. Irizarry RA, Hobbs B, Collin F, Beazer-Barclay YD, Antonellis KJ, et al. Exploration, normalization, and summaries of high density oligonucleotide array probe level data. Biostatistics. 2003; 4:249–264. [PubMed: 12925520]
23. Cho YJ, Tsherniak A, Tamayo P, Santagata S, Ligon A, et al. Integrative genomic analysis of medulloblastoma identifies a molecular subgroup that drives poor clinical outcome. J Clin Oncol. 2011; 29:1424–1430. [PubMed: 21098324]
24. Northcott PA, Hielscher T, Dubuc A, Mack S, Shih D, et al. Pediatric and adult sonic hedgehog medulloblastomas are clinically and molecularly distinct. Acta Neuropathol. 2011; 122:231–240. [PubMed: 21681522]
25. Holen H, Shadidi M, Narvhus K, Kjøsnes O, Tierens A, et al. Signaling through ephrin-A ligand leads to activation of Src-family kinases, Akt phosphorylation, and inhibition of antigen receptor-induced apoptosis. J Leukoc Biol. 2008; 84:1183–1191. [PubMed: 18593733]
26. Zisch AH, Kalo MS, Chong LD, Pasquale EB. Complex formation between EphB2 and Src requires phosphorylation of tyrosine 611 in the EphB2 juxtamembrane region. Oncogene. 1998; 16:2657–2670. [PubMed: 9632142]
27. Nakada M, Hayashi Y, Hamada J. Role of Eph/ephrin tyrosine kinase in malignant glioma. Neuro Oncol. 2011; 13:1163–1170. [PubMed: 21856686]
28. Johnson RA, Wright KD, Poppleton H, Mohankumar KM, Finkelstein D, et al. Cross-species genomics matches driver mutations and cell compartments to model ependymoma. Nature. 2010; 466:632–636. [PubMed: 20639864]
29. Jiang G, Freywald T, Webster J, Kozan D, Geyer R, et al. In human leukemia cells ephrin-B-induced invasive activity is supported by Lck and is associated with reassembling of lipid raft signaling complexes. Mol Cancer Res. 2008; 6:291–305. [PubMed: 18314490]
30. Tanaka M, Kamata R, Takigahira M, Yanagihara K, Sakai R. Phosphorylation of ephrin-B1 regulates dissemination of gastric scirrhous carcinoma. Am J Pathol. 2007; 171:68–78. [PubMed: 17591954]
31. Tanaka M, Sasaki K, Kamata R, Sakai R. The C-terminus of ephrin-B1 regulates metalloproteinase secretion and invasion of cancer cells. J Cell Sci. 2007; 120:2179–2189. [PubMed: 17567680]

32. Tanaka M, Kamata R, Sakai R. Phosphorylation of ephrin-B1 via the interaction with claudin following cell-cell contact formation. EMBO J. 2005; 24:3700–3711. [PubMed: 16211011]

33. Nakada M, Drake KL, Nakada S, Niska JA, Berens ME. Ephrin-B3 ligand promotes glioma invasion through activation of Rac1. Cancer Res. 2006; 66:8492–8500. [PubMed: 16951161]

34. Cortina C, Palomo-Ponce S, Iglesias M, Fernández-Masip JL, Vivancos A, et al. EphB-ephrin-B interactions suppress colorectal cancer progression by compartmentalizing tumor cells. Nat Genet. 2007; 39:1376–1383. [PubMed: 17906625]

35. Chiu ST, Chang KJ, Ting CH, Shen HC, Li H, et al. Over-expression of EphB3 enhances cell-cell contacts and suppresses tumor growth in HT-29 human colon cancer cells. Carcinogenesis. 2009; 30:1475–1486. [PubMed: 19483190]

36. Lee HS, Nishanian TG, Mood K, Bong YS, Daar IO. EphrinB1 controls cell-cell junctions through the Par polarity complex. Nat Cell Biol. 2008; 10:979–986. [PubMed: 18604196]

37. Bong YS, Lee HS, Carim-Todd L, Mood K, Nishanian TG, et al. EphrinB1 signals from the cell surface to the nucleus by recruitment of STAT3. Proc Natl Acad Sci U S A. 2007; 104:17305–17310. [PubMed: 17954917]

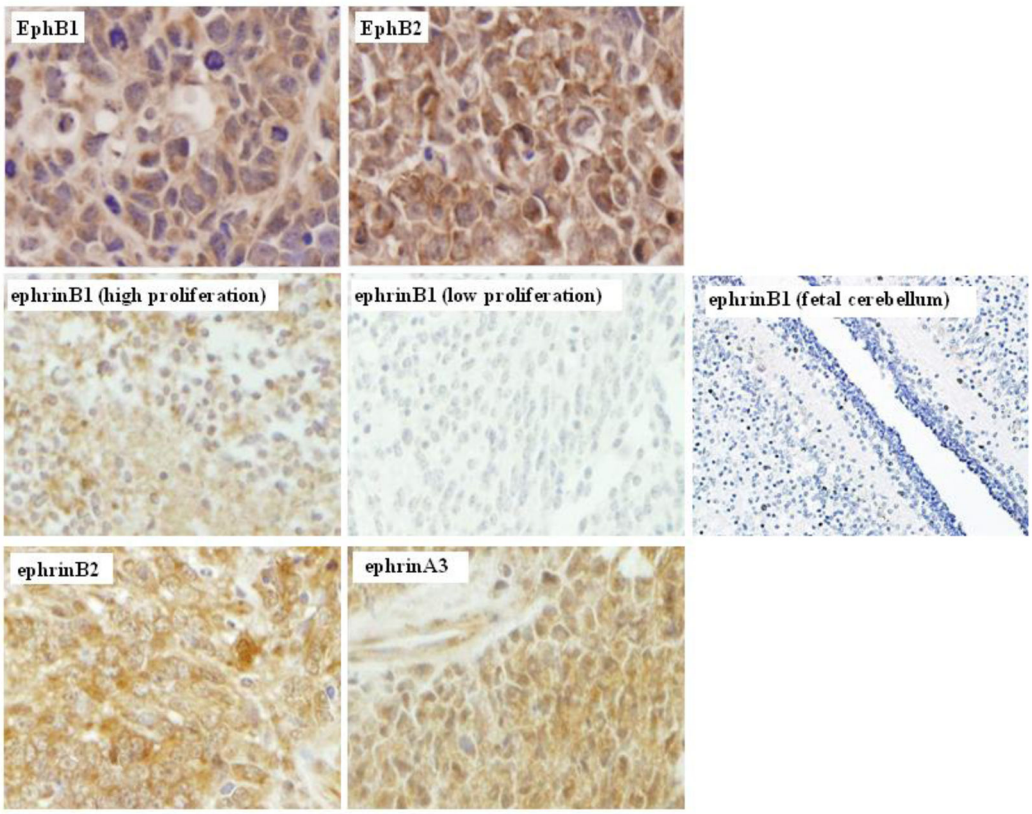

Fig. 1.

EphrinB1 is differentially expressed in childhood medulloblastoma (MB). Representative photomicrographs (40X) for immunohistochemistry of MB tissue demonstrate strong diffuse cytoplasmic and membrane positive immunostaining for EphB1, EphB2, ephrinB2 and ephrinA3. In contrast, positive immunostaining for ephrinB1 is restricted to islands within the tumor comprised of dense neoplastic cells with a higher mitotic proliferative index (far left middle panel). EphrinB1 immunostaining is negative in the less densely cellular neoplastic regions displaying a lower mitotic index within the same tumor (center middle panel) and is negative in normal fetal cerebellum (far right middle panel)

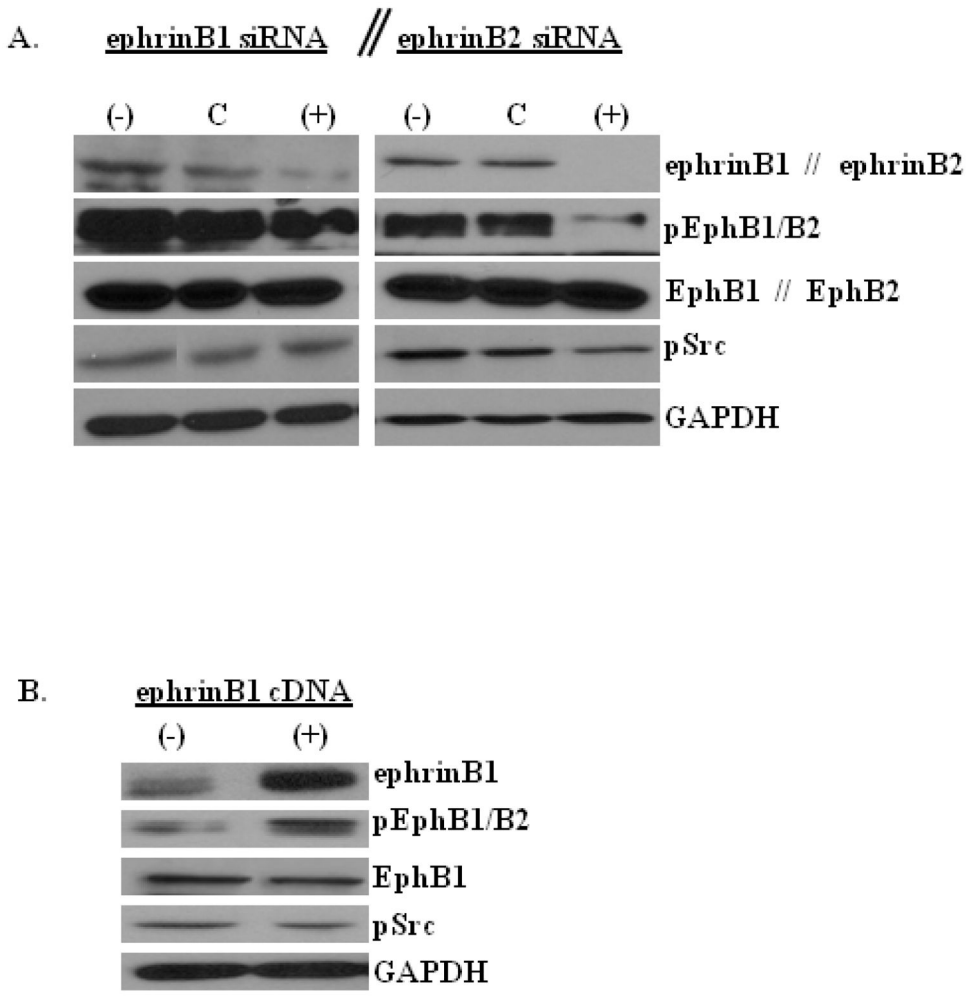

Fig. 2.

EphrinB1 and ephrinB2 differentially regulate EphB1/B2 and Src activation. Representative phospho-specific and total protein Western blots of whole cell lysates of D556 native control MB cells (−) or D556 cells transfected with negative control siRNA (NC), ephrinB1 siRNA (+), ephrinB2 siRNA (+), or ephrinB1 cDNA (+), as indicated. GAPDH serves as internal protein loading control in each experiment. **a)** EphrinB1 knockdown (left panels) results in a modest decrease in the level of EphB1/B2 phosphorylation (forward signaling), but does not alter the level of Src phosphorylation (reverse signaling). EphrinB2 knockdown (right panels) results in a marked decrease in the level of EphB1/B2 and Src phosphorylation. **b)** EphrinB1 overexpression results in a modest increase in the level of EphB1/B2 phosphorylation, but does not alter the level of Src phosphorylation or total protein expression of EphB1

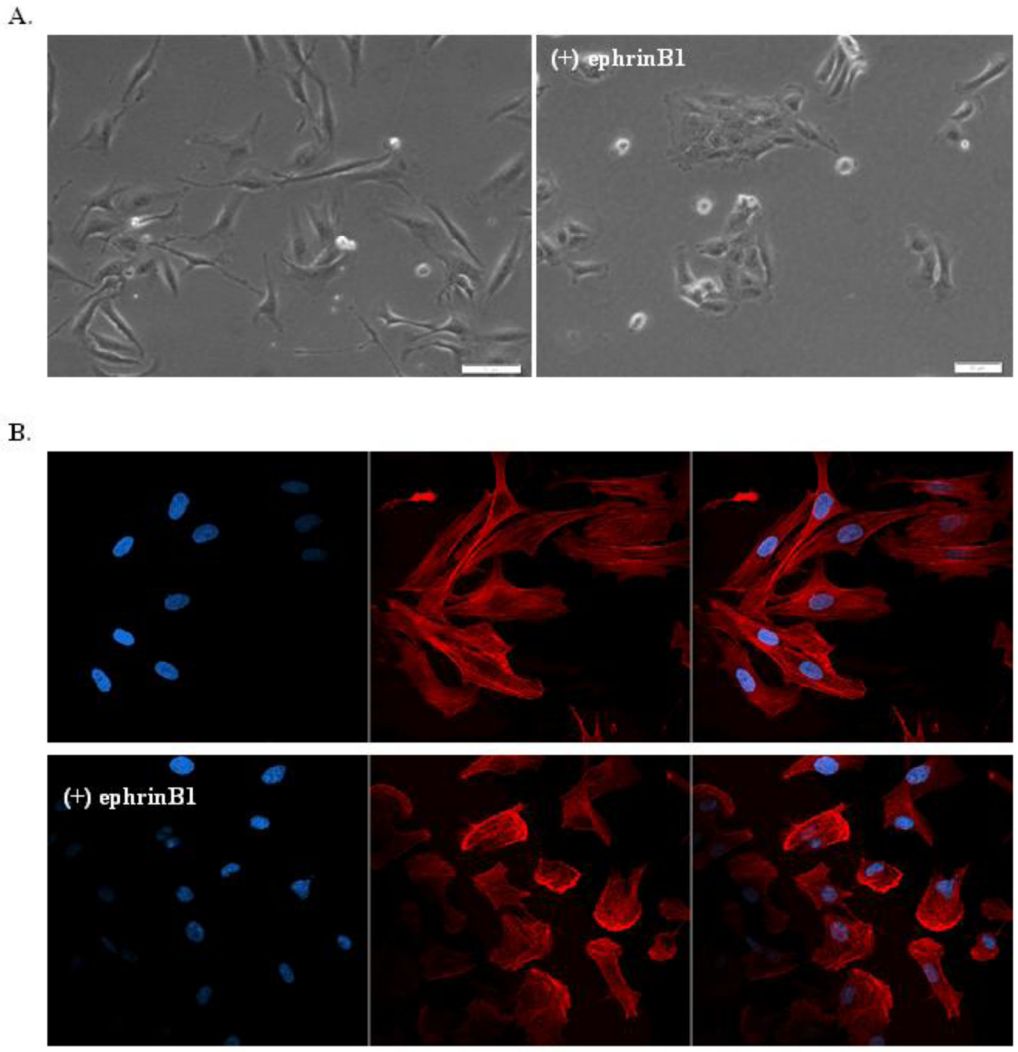

Fig. 3.

EphrinB1 signaling regulates cell morphology and F-actin distribution.

Representative photomicrographs (40X) of D556 native control cells compared to D556-ephrinB1 stable overexpressing cells grown on fibronectin. **a)** Under light microscopy, D556 control cells (left panel) spread out in monolayers and form long filamentous cell-cell contacts, while D556-ephrinB1 overexpressing cells (right panel) demonstrate contracted morphology and growth in segregated colonies. **b)** Under fluorescence microscopy, immunostaining for nuclear DNA (DAPI, blue, left panel), F-actin (phalloidin, red, middle panel) and merged (right panel) demonstrates that D556 control cells (upper panel row) have symmetrically aligned F-actin within long filamentous cellular protrusions, while D556-ephrinB1 overexpressing cells (lower panel row) have rounded morphology, reduced cell-cell contacts and decreased sites of cell adhesion, with F-actin concentrated primarily in the periphery of the cell membrane

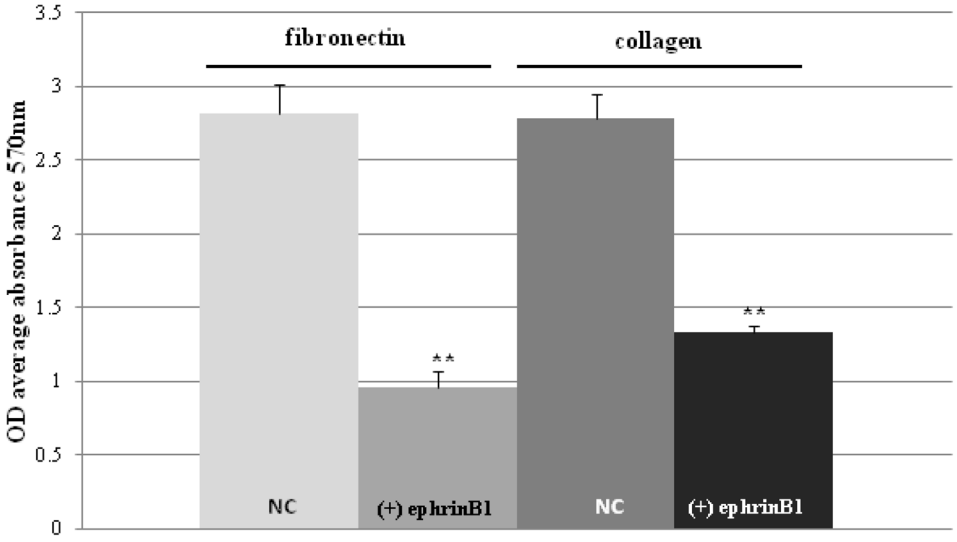

Fig. 4.

EphrinB1 overexpression inhibits MB cell adhesion to fibronectin and collagen.

Graph of cell adhesion assay results demonstrate that D556-ephrinB1 stable overexpressing cells ((+) ephrinB1) have significantly reduced adhesion to fibronectin and collagen in comparison to D556 native control cells (NC), as measured by OD average absorbance at 570 nm. Bars represent the mean ± SD of 3 separate experiments ($^{**}P<0.001$)

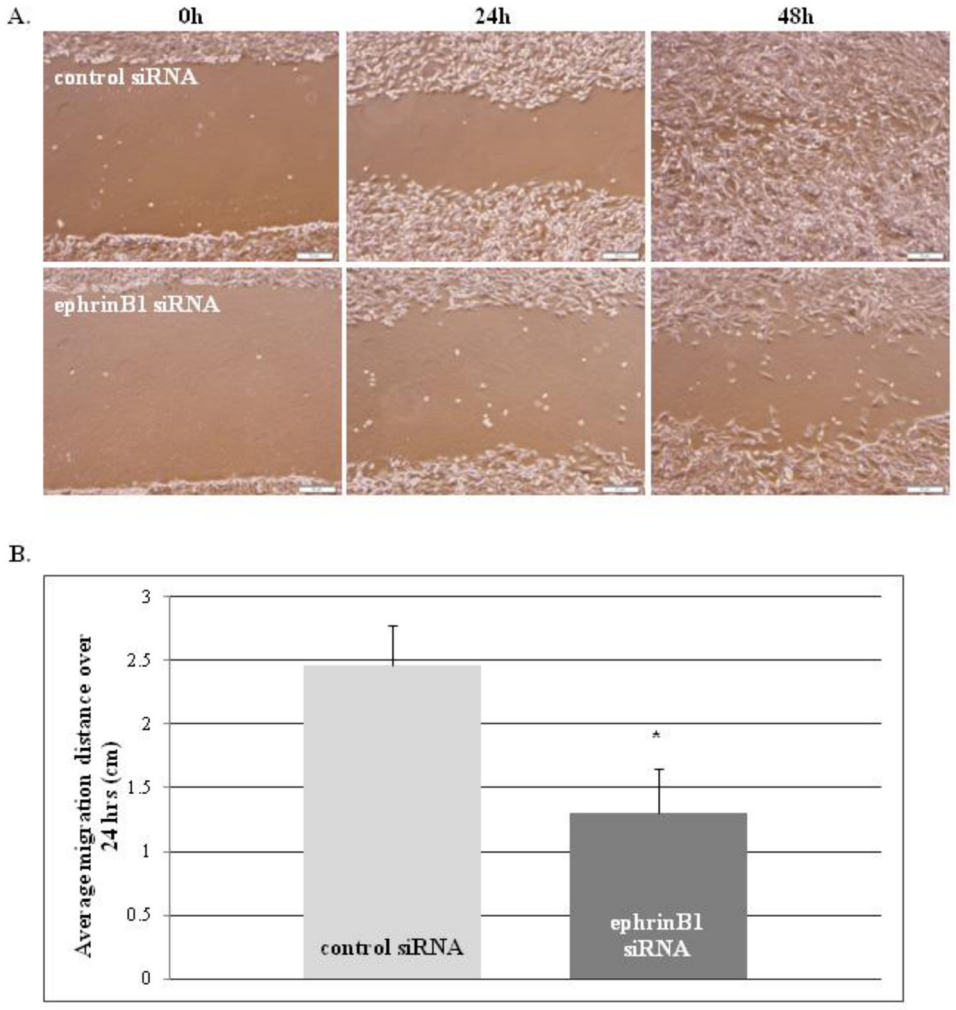

Fig. 5.

EphrinB1 knockdown inhibits MB cell migration.

Scratch assay results of D556 cells transfected with negative control siRNA or ephrinB1 siRNA at 0, 24 and 48 h time points after scratch induced. **a)** Representative photomicrographs (10X) of scratch assay under light microscopy at the indicated time points show that ephrinB1 knockdown cells are impaired in their ability to migrate inwards to fill in the scratch at 24 and 48 h compared to negative control cells. **b)** Graph of the average distance migrated in cm over 24 h in scratch assays demonstrates that ephrinB1 knockdown cells have significantly decreased migration in comparison to negative control cells. Bars represent the mean ± SD of 3 separate experiments ($^{*}P$=0.01)